



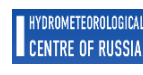
WORLD  
METEOROLOGICAL  
ORGANIZATION



# GLOBAL SEASONAL CLIMATE UPDATE

TARGET SEASON: December-January-February 2023-2024

Issued: 26 November 2023



## Summary

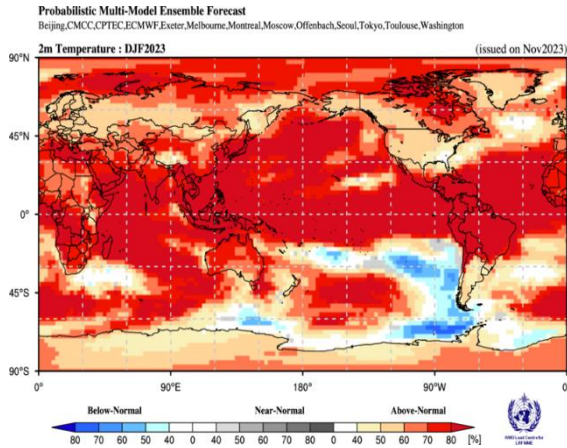
During August-September 2023, the Pacific Niño sea-surface temperature (SST) index in the eastern Pacific (Niño 1+2) was much above-normal and the other three indices in the central Pacific were also above-normal. The observed SST conditions in the equatorial Pacific were characterized by an El Niño state. The observed Indian Ocean Dipole (IOD) was also above-normal. The North Tropical Atlantic (NTA) SST index was above-normal and reflected widespread warmth in the tropical Atlantic north of the equator. The South Tropical Atlantic (STA) SST index was positive but near-normal.

Above-normal sea-surface temperature anomalies in the Niño 3.4 and Niño 3 regions are predicted to continue during the December-February (DJF) 2023/24 season, indicating the continuation of moderate to strong El Niño conditions. Farther west in the Niño 4 region, the sea-surface temperature anomaly is also predicted to be above-normal. The strength of the Indian Ocean Dipole (IOD) index is predicted to decline but stay above-normal in DJF 2023/24. In the equatorial Atlantic, SSTs are predicted to be above-normal in both the northern (NTA) and the southern (STA) areas during the season.

Consistent with the anticipated El Niño in the equatorial central and eastern Pacific, together with the prediction of above-normal sea-surface temperatures over much of the global oceans, there is widespread prediction of above-normal temperatures over almost all land areas. Positive temperature anomalies are expected over almost the entire Northern Hemisphere except in the far south-eastern part of North America and over a small area of equatorial East Africa. The predicted anomalies in the Northern Hemisphere are larger in high latitudes, but the largest increases in probabilities for above-normal temperatures are generally south of about 40° N over Europe, Africa and Asia, and south of about 30° N over Central America. However, around the Sea of Okhotsk, and in a small area north of the Himalayas, the probabilities for above-normal temperature are only weakly enhanced. Over much of North America, with the exception of the far south-east, and over Greenland probabilities for above-normal temperature are moderately enhanced, although the increase in probability is higher around the Hudson Bay. In the Caribbean and Central America, the probabilities of above-normal temperatures are strongly increased, and this area extends to about 30° S over South America. Further south, probabilities for above-normal temperatures are weakly increased, and it is only along the west and south coasts that probabilities for below-normal temperature are increased. Over most of the rest of the Southern Hemisphere land areas, temperatures are predicted to experience positive temperature anomalies, as in the Northern Hemisphere. Thus, in Africa south of the equator, including Madagascar and the south-west Indian Ocean north of about 30° S, above-normal temperatures are predicted with high probabilities, although model consistency is high only over Madagascar and neighbouring oceanic areas, and along the west coast of Central and northern Southern Africa. Over Australia above-normal temperatures are again predicted with moderate to high probability, but the probabilities are only weakly increased over New Zealand, and along about 20° S in the Pacific Ocean, there is a narrow band of predicted normal-to-below normal temperatures that expands southwards in the far south-eastern Pacific.

Predictions for rainfall are similar to some of the canonical rainfall impacts of El Niño, which is expected to strengthen in DJF 2023/24. Above-normal rainfall is predicted over a narrow band along and just north of the equator from 150° E extending to the west coast of South America. Probabilities for above-normal rainfall are strongly enhanced in much of this area. However, immediately on and south of the equator between about 165° W and 110° W, enhanced probability for normal rainfall is predicted. Across most of the Pacific Ocean south of about 10° N, and immediately to the north of the wet band and to about 30° N, rainfall is predicted to be below-normal. The northern band of predicted dry extends from the Philippines to the north-west coast of Central America. In the Southern Hemisphere, the area of below-normal rainfall extends westwards across northern and western Australia, where it expands into the central Indian Ocean to about 60° E and is consistent with the prediction for the positive phase of the IOD. Probabilities in these below-normal areas are strongest in the eastern Indian Ocean and in the North Pacific between about 180° and 120° E. For the eastern Maritime continent, an area of above-normal rainfall extends northwards into southeast Asia and expands to cover most of Asia and Europe. In the western Indian Ocean, above-normal rainfall is predicted in a C-shaped area that extends from immediately north of the equator at about 80° E into East Africa, and then south-eastwards across northern Madagascar into the central South Indian Ocean. Probabilities of above-normal rainfall are strongly enhanced over East Africa and the neighbouring ocean. To the south-west, over most of southern Africa, below-normal rainfall is predicted with low to moderately increased probabilities, while much of sub-Saharan Africa north of the equator has increased probabilities of normal precipitation. The dry area over southern Africa, and another dry area in northwest Africa extend across the Atlantic to South America and the southern Caribbean, and much of the continent north of 30° S and east of about 65° W is predicted to be dry with moderately increased probability. Below-normal rainfall is also predicted along the west coast of South America south of about 15° S. There are weak increases in probability for above-normal rainfall over south-eastern and north-western South America. Weak increases in probability for above-normal precipitation are also predicted over most of Asia and Europe, the northern Caribbean, south-east and north-east North America.

## Surface Air Temperature, DJF 2023-2024



## Precipitation, DJF 2023-2024

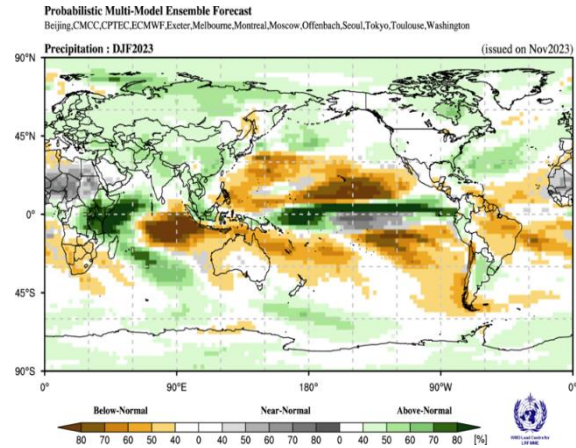


Figure 1. Probabilistic forecasts of surface air temperature and precipitation for the season December-February 2023-2024. The tercile category with the highest forecast probability is indicated by shaded areas. The most likely category for below-normal, above-normal, and near-normal is depicted in blue, red, and grey shadings respectively for temperature, and orange, green and grey shadings respectively for precipitation. White areas indicate equal chances for all categories in both cases. The baseline period is 1993-2009.

### 1. Observations: August-October (ASO) 2023

In the following sections, observed temperature and precipitation patterns for the previous season are discussed. For more detailed information about regional and local climate anomalies, the reader is referred to the concerned WMO Regional Climate Centres (RCCs) or RCC Networks, listed in Section 5.

#### 1.1 Large-scale sea-surface temperature (SST) indices

During August-September 2023, the Pacific Niño sea-surface temperature (SST) index in the eastern Pacific (Niño 1+2) was much above-normal and the other three indices in the central Pacific were also above-normal. The observed SST conditions in the equatorial Pacific were characterized by an El Niño state. The observed Indian Ocean Dipole (IOD) was also above-normal. The North Tropical Atlantic (NTA) SST index was above-normal and reflected widespread warmth in the tropical Atlantic north of the equator. The South Tropical Atlantic (STA) SST index was positive but near-normal.

Month	Niño 1+2	Niño 3	Niño 4	Niño 3.4	IOD	NTA	STA
August 2023	3.3	1.6	2.0	1.3	0.7	1.3	0.4
September 2023	2.8	2.0	2.1	1.5	0.8	1.3	0.3
October 2023	2.5	2.1	2.0	1.6	1.4	1.1	0.1
August-October 2023	2.9	1.9	2.0	1.5	1.0	1.2	0.3

Table 1. Large-scale oceanic indices (°C). Anomalies are with respect to the 1991-2020 average. (Source: U.S. Climate Prediction Center)

## 1.2 Observed temperature

Over land areas, temperature anomalies for August-October 2023 were generally above normal with small regions of below-normal conditions interspersed in between (Figure 2, top). In the northern hemisphere, the largest positive land-temperature anomalies occurred over southern and western Europe, northern Asia and parts of eastern Asia, northern regions of North America, and the northern regions of Central America extending into southwest Northern America. In the southern hemisphere, positive land-temperature anomalies occurred over north of 30°N in South America, below the equator in Africa, western and eastern regions of Australia, and New Zealand. Small regions with negative temperature anomalies were observed over the eastern regions of Greenland, interior regions of western Africa, south of 35°S over South America, extreme northwest South America, extreme northwest North America, and Madagascar.

Over the oceans, in the equatorial eastern Pacific extending all the way to the western coastal regions of South America, extending further north along the coast of Central America and south along the coast of South America, above-normal temperature anomalies occurred. These temperature anomalies reflected El Niño conditions. In the extratropical southern Pacific Ocean between 60°-30° S and between 120°-60° W, below average temperatures were observed. SST anomalies in the Pacific north of 30° N and in the southern Pacific along 45° S were positive. SSTs in the eastern Indian Ocean were below-normal while above-normal temperature dominated in the western Indian Ocean and indicated a positive phase of the Indian Ocean Dipole. SSTs in the Gulf of Mexico, Caribbean and over almost the entire Atlantic Ocean and Mediterranean were above-normal.

Warm extremes (exceeding all seasonal mean temperatures observed during 1991-2020), occurred over northern regions of Central America extending into southwest North America, the Caribbean, parts of northern regions and northeastern North America, regions north of 30°S in South America, equatorial Africa extending into the coastal regions of western Africa, regions of southern and western Europe, parts of eastern Asia extending Japan, and western Australia. A small region of cold extreme was observed in the interior region of western Africa. Warm extremes also occurred over oceanic regions, notably over the eastern Atlantic extending from the coastal regions from north-western Africa into the coastal regions of western Europe and over the northeast Pacific Ocean.

## 1.2 Observed precipitation

For August-September 2023, the precipitation anomalies in the equatorial Pacific reflected spatial pattern consistent with El Niño conditions with a narrow band of above-normal anomalies extending throughout the equatorial eastern Pacific and a broader region in the western Pacific (Figure 3, top panel). To the north of this equatorial band of above-normal anomalies, starting near the Date Line a band of below-normal precipitation anomalies extended eastward towards Central America into the Gulf of Mexico. South of the equator, also starting near the date line, a band of above-normal precipitation anomalies extended south-eastward to 120°W and was flanked by below-normal rainfall on both sides. Associated with the positive phase of IOD, below-normal precipitation anomalies dominated the eastern half of the Indian ocean. Positive precipitation anomalies occurred in the north equatorial Atlantic. Coastal regions of western and eastern Australia were dominated by below-normal precipitation anomalies.

Over land, negative precipitation anomalies dominated in Central America and extended into the northern regions of South America. Below-normal precipitation anomalies extended along 60°N across North America extending into southern Greenland. Below-normal rainfall anomalies occurred over southern Europe, and the southern region of the Indian subcontinent. Positive rainfall anomalies were observed over the western region of southern Europe and extended along the coastal region of western Europe to Northern Europe. Below-normal rainfall anomalies occurred over the eastern half of Australia.

Regions of dry extremes (drier than all seasonal mean rainfall observed during 1991-2020) occurred over parts of central America, northeast North America, southeastern Greenland. No regions with systematic wet extremes were observed.

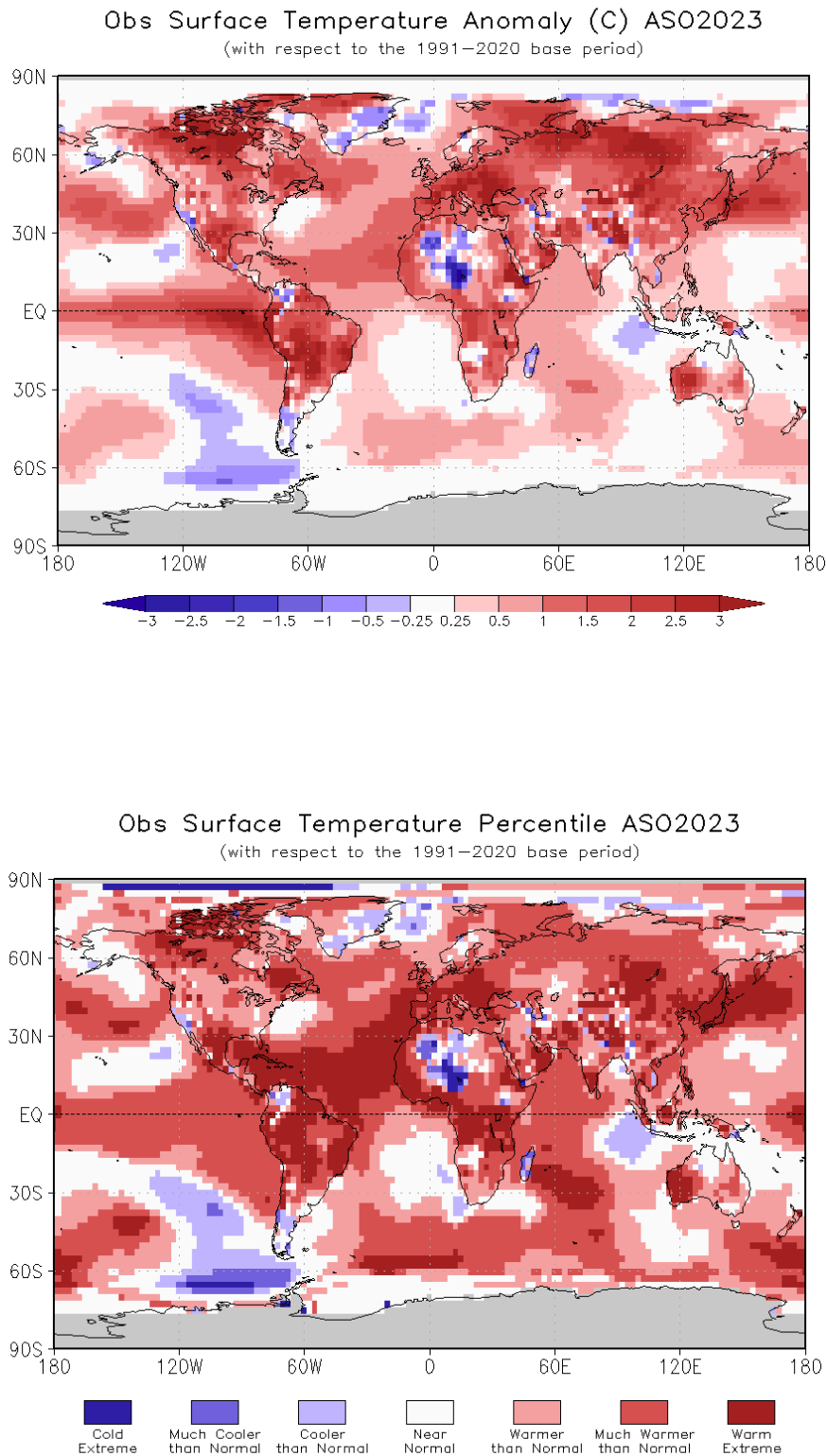


Figure 2. Observed August-October 2023 near-surface temperature anomalies relative to 1991-2020 (top). The *Cooler than Normal*, *Near Normal*, and *Warmer than Normal* shadings on the percentile map (bottom) indicate that seasonal mean anomalies were in the bottom, middle, and upper tercile of the 1991-2020 distribution, respectively. Regions with anomalies in the lowest and highest decile (or 10%) of the distribution are marked as *Much Cooler than Normal* and *Much Warmer than Normal*, respectively. The *Cold Extreme* and *Warm Extreme* shadings indicate that the anomalies exceeded the coldest and warmest temperature values of the 1991-2020 period for the season. Grey shading indicates areas where observational analysis was not available. (Source: U.S. Climate Prediction Center).

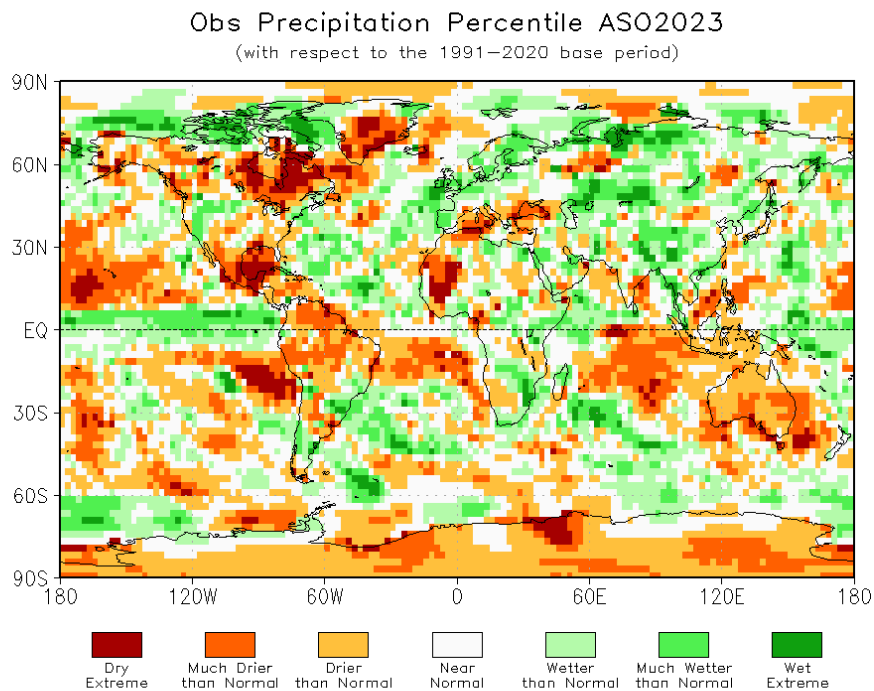
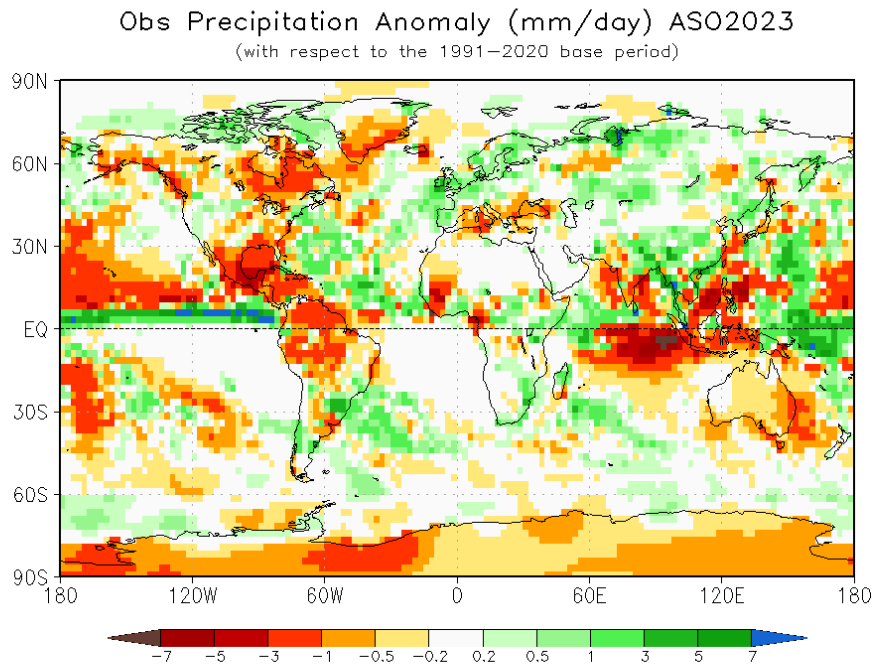


Figure 3. Observed precipitation anomalies for August–October 2023, relative to 1991–2020 base period (top). The *Drier than Normal*, *Near Normal* and *Wetter than Normal* shadings on the percentile map (bottom) indicate that seasonal mean anomalies were in the bottom, middle, and upper tercile of the 1991–2020 distribution, respectively. Regions with anomalies in the lowest and highest decile (or 10%) of the distribution are marked as *Much Drier than Normal* and *Much Wetter than Normal*, respectively. The *Dry Extreme* and *Wet Extreme* shadings indicate that the anomalies exceeded the driest and wettest values of the 1991–2020 period for the season.

(Source: U.S. Climate Prediction Center).

## 2. Potential evolution of the state of the climate over the next three months (December-February 2023-2024)

### 2.1 Large-scale SST-based indices, December - February (DJF) 2023-2024

Month	Nino 1+2	Nino 3	Nino 4	Nino3.4	IOD	NTA	STA
<b>December 2023</b>	1.7±0.4	2.1±0.4	1.5±0.2	2.0±0.3	1.2±0.2	0.9±0.1	0.5±0.3
<b>January 2024</b>	1.3±0.4	2.1±0.3	1.5±0.2	2.1±0.3	0.7±0.2	0.9±0.1	0.5±0.3
<b>February 2024</b>	1.0±0.3	1.9±0.3	1.4±0.2	1.9±0.3	0.3±0.2	0.9±0.1	0.5±0.3
<b>DJF 2023-2024</b>	1.3±0.4	2.0±0.4	1.5±0.2	2.0±0.3	0.7±0.3	0.9±0.1	0.5±0.3

Table 2: Multi-model forecasts for oceanic indices (°C), with standard deviation. Values are the equal-member-weighting average of those derived, using each GPC model's own hindcast climate mean, from the GPCs supplying SST forecasts (GPC Beijing, CMCC, ECMWF, Exeter, Melbourne, Montreal, Offenbach, Seoul, Tokyo, Toulouse, Washington). The standard deviation is calculated on all ensemble members. The latitude/longitude bounds of the regions are given in the supplementary information section.

Observed sea-surface temperatures in the central tropical Pacific were characterized by El Niño state during August-September 2023. Above-normal sea-surface temperature anomalies in the Niño 3.4 and Niño 3 regions are predicted to continue during the December-February (DJF) 2023/24 season, indicating the continuation of moderate to strong El Niño conditions. Farther west in the Niño 4 region, the sea-surface temperature anomaly is also predicted to be above-normal. The strength of the Indian Ocean Dipole (IOD) index is predicted to decline but stay above-normal in DJF 2023/24. In the equatorial Atlantic, SSTs are predicted to be above-normal in both the northern (NTA) and the southern (STA) areas during the season.

### 2.2 Predicted temperature, December - February 2023-2024

For information on the construction of the multi-model forecast maps, refer to the supplementary information section. (Note: Maps indicating forecast consistency among GPC models are available in the supplementary information<sup>1</sup>).

---

<sup>1</sup> File with supplementary information can be downloaded from [https://ftp.cpc.ncep.noaa.gov/mingyue/GSCUWMO/Forecasts/GSCU\\_DJF2023\\_supplementary\\_info\\_LC-LRFMME.docx](https://ftp.cpc.ncep.noaa.gov/mingyue/GSCUWMO/Forecasts/GSCU_DJF2023_supplementary_info_LC-LRFMME.docx)

**Probabilistic Multi-Model Ensemble Forecast**

Beijing, CMCC, CPTEC, ECMWF, Exeter, Melbourne, Montreal, Moscow, Offenbach, Seoul, Tokyo, Toulouse, Washington

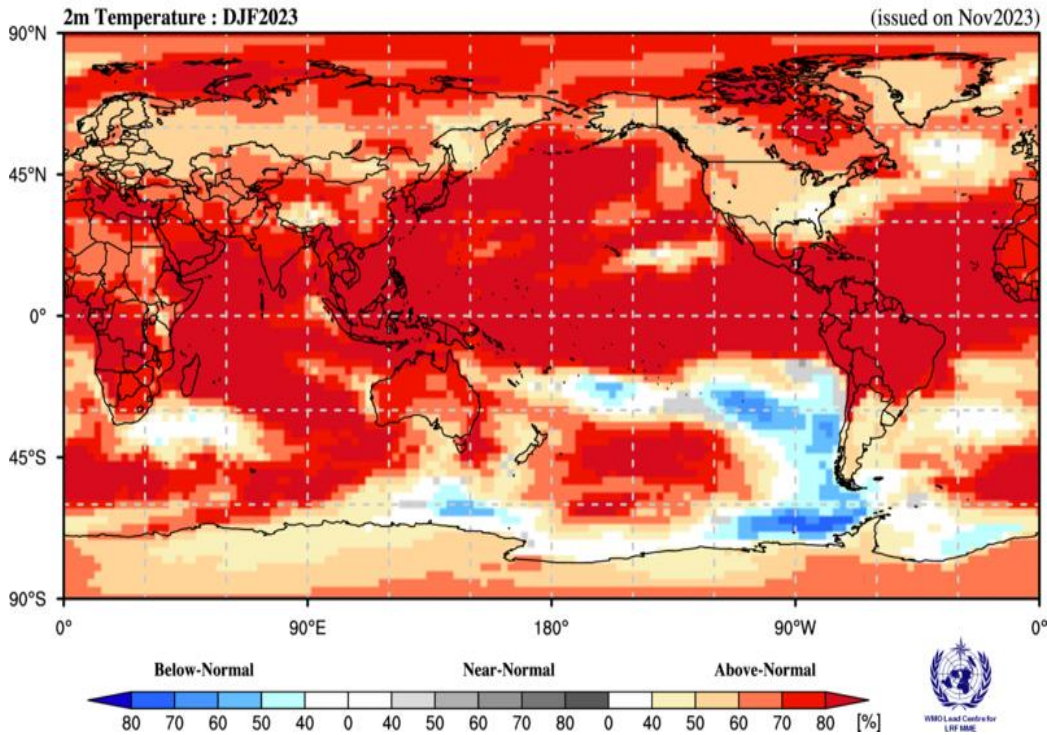


Figure 4. Probabilistic forecasts of surface air temperature for December-February 2023-2024. The tercile category with the highest forecast probability is indicated by shaded areas. The most likely category for below-normal, above-normal, and near-normal is depicted in blue, red, and grey shadings, respectively. White areas indicate equal chances for all categories in both cases. The baseline period is 1993-2009. Figure is generated by The WMO Lead Centre for Long-Range Forecast Multi-Model Ensemble.

Consistent with the anticipated El Niño in the equatorial central and eastern Pacific, together with the prediction of above-normal sea-surface temperatures over much of the global oceans, there is widespread prediction of above-normal temperatures over almost all land areas. Positive temperature anomalies are expected over almost the entire Northern Hemisphere except in the far south-eastern part of North America and over a small area of equatorial East Africa. The predicted anomalies in the Northern Hemisphere are larger in high latitudes, but the largest increases in probabilities for above-normal temperatures are generally south of about 40° N over Europe, Africa and Asia, and south of about 30° N over Central America. However, around the Sea of Okhotsk, and in a small area north of the Himalayas, the probabilities for above-normal temperature are only weakly enhanced. Over much of North America, with the exception of the far south-east, and over Greenland probabilities for above-normal temperature are moderately enhanced, although the increase in probability is higher around the Hudson Bay. In the Caribbean and Central America, the probabilities of above-normal temperatures are strongly increased, and this area extends to about 30° S over South America. Further south, probabilities for above-normal temperatures are weakly increased, and it is only along the west and south coasts that probabilities for below-normal temperatures are increased. Over most of the rest of the Southern Hemisphere land areas, temperatures are predicted to experience positive temperature anomalies, as in the Northern Hemisphere. Thus, in Africa south of the equator, including Madagascar and the south-west Indian Ocean north of about 30° S, above-normal temperatures are predicted with high probabilities, although model consistency is high only over Madagascar and neighbouring oceanic areas, and along the west coast of Central and northern Southern Africa. Over Australia above-normal temperatures are again predicted with moderate to high probability, but the probabilities are only weakly increased over New Zealand, and along about 20° S in the Pacific Ocean, there is a narrow band of predicted normal-to-below normal temperatures that expands southwards in the far south-eastern Pacific.



RA I (Africa): Enhanced probabilities of above-normal temperatures are indicated over all of mainland Africa and Madagascar. The probability increases are strong everywhere except over a small area of equatorial East Africa. Model consistency is strong over North Africa, along the south coast of West Africa and extending along the west coast of Central Africa to about 15° S, and over Madagascar and ocean areas to the north and east. Over the rest of the mainland, model consistency is moderate, except over the area of equatorial East Africa.

RA II (Asia): Enhanced probabilities for above-normal temperatures are indicated over all of mainland Asia, and model consistency is high almost everywhere, with the exception of an area in the vicinity of the Himalayas, another area around the Sea of Okhotsk, and a narrow band in East Asia along about 50° N. Despite the strong to moderate model consistency, probabilities for above-normal temperatures are high only along the Arctic coast, all areas south of about 30° S, and extending northwards over the Pacific Ocean to Japan. Across most of the continent at about 60° N, the probabilities of above-normal are only weakly enhanced.

RA III (South America): Strongly enhanced probabilities for above-normal temperatures are indicated over South America north of about 30° S. Model consistency is high over this region. Further south, there is a weak increase in the probability for above-normal temperature, except immediately off the west and south coasts where below-normal temperatures are predicted with weak to moderate probability. Weak to moderate model consistency reflect the weak shifts in probabilities in both the areas of predicted positive and negative temperature anomalies of southern South America.

RA IV (North America, Central America, and the Caribbean): There are enhanced probabilities for above-normal temperatures over most of North America, with the exception of the south-east mainland where there is no clear signal. The probabilities for above-normal temperatures are strong over Central America and the Caribbean south of about 25° N, moderate to strong extending around the Hudson Bay, and weak over the rest of the continent. Probabilities for above-normal temperature are also strong along much of the Pacific coast, and over most of the North Pacific Ocean as a whole, with the exception of a narrow band along 20° N from about 150° to 120° W.

RA V (Southwest Pacific): Strongly enhanced probabilities for above-normal temperatures are predicted across the whole of the Pacific Ocean north of about 15° S, and again between about 30° and 60° S in the central part of the South Pacific. These probabilities weaken over New Zealand but strengthen again over Australia. Further south, there are patches where probabilities for above-normal temperature are also strongly increased, including a large area extending from south of Australia, around New Zealand to about 120° W. Model consistency is high along the equator and along about 40° S, and is moderate over Australia. Over the south-eastern Pacific off the west coast of South America there is an area of weak to moderately enhanced probabilities of below-normal temperature, with a weak band extending along about 25° S to about the Date Line. Model consistency is high in this anomalously cold area only in small areas in the south-eastern Pacific.

RA VI (Europe): The probabilities for above-normal temperatures are increased over all of Europe with stronger probabilities over the Mediterranean. The model-to-model consistency is high almost everywhere.

## 2.3 Predicted precipitation, December - February 2023-2024

**Probabilistic Multi-Model Ensemble Forecast**

Beijing,CMCC,CPTEC,ECMWF,Exeter,Melbourne,Montreal,Moscow,Offenbach,Seoul,Tokyo,Toulouse,Washington

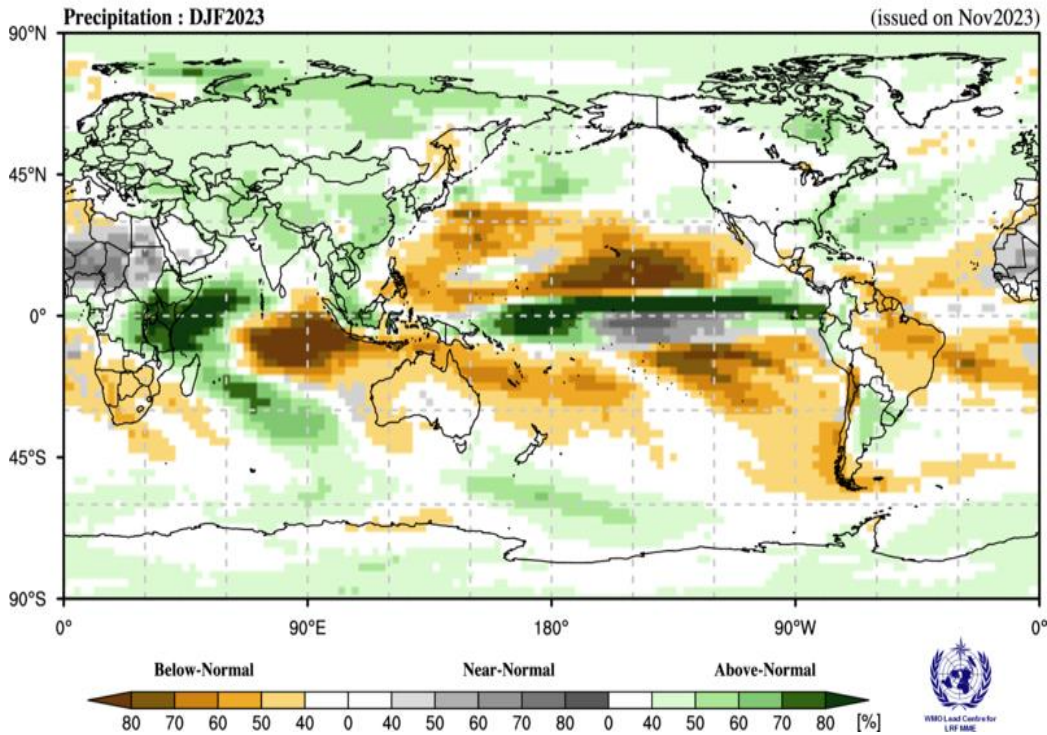


Figure 5. Probabilistic forecasts of precipitation for the season for December-February 2023-2024. The tercile category with the highest forecast probability is indicated by shaded areas. The most likely category for below-normal, above-normal, and near-normal is depicted in orange, green and grey shadings, respectively. White areas indicate equal chances for all categories in both cases. The baseline period is 1993-2009. Figure is generated by The WMO Lead Centre for Long-Range Forecast Multi-Model Ensemble.

Predictions for rainfall are similar to some of the canonical rainfall impacts of El Niño, which is expected to strengthen in DJF 2023/24. Above-normal rainfall is predicted over a narrow band along and just north of the equator from 150° E extending to the west coast of South America. Probabilities for above-normal rainfall are strongly enhanced in much of this area. However, immediately on and south of the equator between about 165° W and 110° W, enhanced probability for normal rainfall is predicted. Across most of the Pacific Ocean south of about 10° N, and immediately to the north of the wet band and to about 30° N, rainfall is predicted to be below-normal. The northern band of predicted dry extends from the Philippines to the north-west coast of Central America. In the Southern Hemisphere, the area of below-normal rainfall extends westwards across northern and western Australia, where it expands into the central Indian Ocean to about 60° E and is consistent with the prediction for the positive phase of the IOD. Probabilities in these below-normal areas are strongest in the eastern Indian Ocean and in the North Pacific between about 180° and 120° E. For the eastern Maritime continent, an area of above-normal rainfall extends northwards into southeast Asia and expands to cover most of Asia and Europe. In the western Indian Ocean, above-normal rainfall is predicted in a C-shaped area that extends from immediately north of the equator at about 80° E into East Africa, and then south-eastwards across northern Madagascar into the central South Indian Ocean. Probabilities of above-normal rainfall are strongly enhanced over East Africa and the neighbouring ocean. To the south-west, over most of southern Africa, below-normal rainfall is predicted with low to moderately increased probabilities, while much of sub-Saharan Africa north of the equator has increased probabilities of normal precipitation. The dry area over southern Africa, and another dry area in northwest Africa extend across the Atlantic to South America and the southern Caribbean, and much of the continent north of 30° S and east of about 65° W is predicted to be dry with weak to moderately increased probability. Below-normal rainfall is also predicted along the west coast of South America south of about 15° S. There are weak increases in probability for above-normal rainfall over south-eastern and north-western South America. Weak increases in probability for above-normal precipitation are also predicted over most of Asia and Europe, the northern Caribbean, south-east and north-east North America.

RA I (Africa): Enhanced probabilities for above-normal precipitation are predicted over much of eastern Africa including the Greater Horn of Africa, and extending into part of Central Africa, and model consistency is moderate to high. This wet area extends to the southeast over northern Madagascar and into the central South Indian Ocean. Over much of southern Africa there are weak increases in the probability of below-normal rainfall, with weak to moderate consistency. Across much of the Sahara, the increased probabilities for normal rainfall largely reflect the aridity of the area and time of year. Over north-west Africa, the probabilities for below-normal rainfall are weakly increased and model consistency is low.

RA II (Asia): A weak enhancement in probability for above-normal precipitation occurs over almost all of Asia with the exception of the Arabian Peninsula and a small area to the east of the Sea of Okhotsk. Model consistency is patchy but mostly moderate. The area of predicted wet conditions extends over the western part of the Maritime Continent, where the probabilities are moderately increased and model consistency is moderate. However, an area over the Philippines as well as a band immediately south of the equator are predicted to be anomalously dry. Model consistency is moderate in these dry areas, except over the eastern Indian Ocean where consistency is strong, and probabilities for below-normal are high.

RA III (South America): South America north of 30° S and east of about 65° W is predicted to be dry with weak to moderately increased probability. Model consistency is highest in the north-west. Below-normal rainfall is also predicted along the west coast of South America south of about 15° S, extending across the southernmost part of the continent. Probabilities are moderately enhanced and model consistency is strong. There are weak increases in probability for above-normal rainfall over south-eastern South America, and model consistency is moderate. There are also weak indications of above-normal rainfall over north-western South America, but the probabilities are strong along the equator at the Pacific coast.

RA IV (North America, Central America, and the Caribbean): There are weak and patchy enhancements in the probabilities for below-normal rainfall in the southern regions of Central America extending into the southern Caribbean. Over the northern Caribbean and extending into south-eastern North America and along much of the east coast, the probabilities are increased for above-normal precipitation and model consistency is moderate to high. Increases in probability of above-normal rainfall are also located in northeast North America, with strongest probabilities over the Hudson Bay, but with moderate model consistency. Weak probabilities of above-normal rainfall are indicated in a small part of western North America, and model consistency is moderate. Over much of the rest of North America there is no clear signal.

RA V (Southwest Pacific): Probabilities for above-normal rainfall are strongly enhanced over a narrow area extending along or immediately north of the equator from about 150° E to the coast of South America. Model consistency is high. Immediately on and a few degrees south of the equator between about 165° W and 110° W, normal rainfall is predicted. Immediately to the north of the equatorial wet band is an area centered at about 150° W, where probabilities for below-normal rainfall are predicted to be strongly increased. This area spans from the Philippines across most of the North Pacific south of about 30° N. Model consistency is strongest east of the Date Line. South of the equator below normal rainfall is also predicted across much of the South Pacific, but with a narrow north-west to south-east band centered at about 150° W. The eastern dry area extends to the west coast of South America, and the western dry area extends over northern and western Australia. Moderate consistency is moderate to high. The predicted dryness over Australia expands into the central Indian Ocean to about 60° E and is consistent with the prediction for the positive phase of the IOD. Probabilities and model consistency in these below-normal areas are strongest in the eastern Indian Ocean. Further south, extending from south of Tasmania, across the southern tip of New Zealand, to beyond 150° W, there is an area with weakly enhanced probabilities of above-normal precipitation, with moderate to strong model consistency.

RA VI (Europe): Most of Europe has weakly enhanced probabilities of above-normal precipitation signal and moderate model consistency.

### 3. Latest updates for monitoring and prediction information

Each month, the latest updates for the real-time monitoring and seasonal mean predictions included in GSCU can be found at:

Monitoring:

<https://ftp.cpc.ncep.noaa.gov/mingyue/GSCUWMO/>

Predictions:

[www.wmolc.org/board/downloadExt?fn=WMOLC\\_T2M.png](http://www.wmolc.org/board/downloadExt?fn=WMOLC_T2M.png)

[http://www.wmolc.org/board/downloadExt?fn=WMOLC\\_PREC.png](http://www.wmolc.org/board/downloadExt?fn=WMOLC_PREC.png)

## 4. How to use the Global Seasonal Climate Update

The GSCU is intended as guidance for RCCs, Regional Climate Outlook Forums (RCOFs) and National Meteorological and Hydrological Services (NMHSs). It does not constitute an official forecast for any region or nation. Seasonal outlooks for any region or nation should be obtained from the relevant RCCs (see below for contact details) or NMHS.

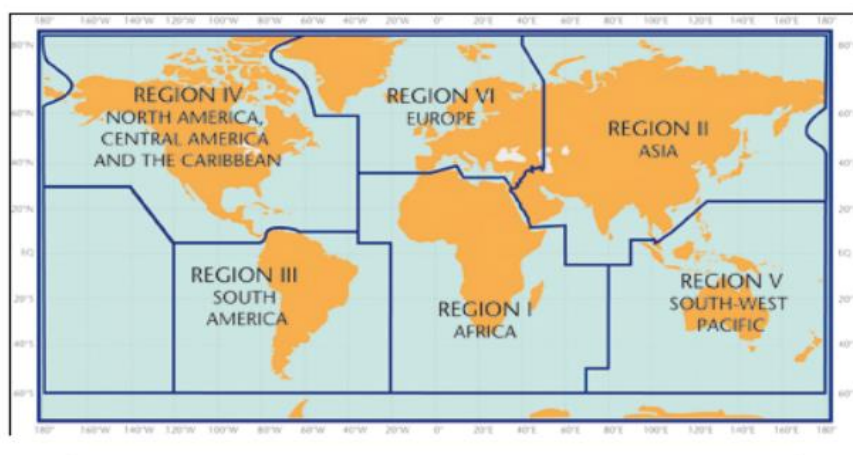
Figure 4 shows the spatial pattern of seasonal mean surface air temperature forecast probabilities. Probabilities are calculated for the average temperature for the season being in the highest third (above-normal or warm), middle third (normal) or lowest third (below-normal or cold) ranges of the baseline record (1993-2009) at each location. Colour code is indicated only for the category that has the highest probability of occurrence. For example, for regions highlighted in red, the most likely forecast category for seasonal mean surface air temperature to occur is warmer than normal. Similarly, the blue colour highlights regions where the seasonal mean surface air temperature forecast indicates the colder than normal category as most likely, while grey colour highlights regions where the seasonal mean temperature forecast indicates the near normal category as most likely. Deeper shades of respective colours highlight increasing probability for the seasonal mean temperature to be in the indicated category. White areas indicate equal chances for all categories.

A particular colour does not assure that the seasonal mean temperature is “certain” to be observed in the most likely forecast category that is shown, but rather its probability of being in that category. As a consequence, the observed seasonal mean temperatures have a non-negligible probability to be observed in a category different from the category indicated on the map as most likely. Users need to take the probabilistic nature of seasonal forecasts into account when making decisions. It should also be noted that the absolute values for the surface air temperature corresponding to the definitions of the above normal (warm), normal or below normal (cold) categories depend on the climatology (historical information) at the location, and therefore, is location dependent.

The interpretation of the probabilities for the rainfall forecast (Figure 5) is the same as that for the seasonal mean surface air temperature except that green and brown colours indicate whether the forecasted seasonal mean precipitation is most likely to be in the wet or dry category. As for surface temperature, grey colour highlights regions where the seasonal mean rainfall forecast indicates the near normal category as the most likely.

The skill of seasonal forecasts is substantially lower than that of weather timescales and skill may vary considerably with region and season. It is important to view the forecast maps together with the skill maps provided in the supplementary material.

For reference, the six WMO Regional Associations domains are depicted in the figure below.



## 5. Designated and developing WMO Regional Climate Centres and Regional Climate Centre Networks

- <https://public.wmo.int/en/our-mandate/climate/regional-climate-centres>

## 6. Resources

Sources for the graphics used in the GSCU:

- The WMO Lead Centre for Long-Range Forecast Multi-Model Ensemble (LC-LRFMME): <http://www.wmolc.org>
- WMO portal to the Global Producing Centres for Long-range Forecasts (GPCs-LRF): <https://public.wmo.int/en/programmes/global-data-processing-and-forecasting-system/global-producing-centres-of-long-range-forecasts>
- WMO portal for Regional Climate Outlook Forums <https://public.wmo.int/en/our-mandate/climate/regional-climate-outlook-products>
- International Research Institute for Climate and Society (IRI): <https://iri.columbia.edu/>
- NOAA Climate Prediction Centre (CPC): <http://www.cpc.ncep.noaa.gov>

## 7. Acknowledgements

This Global Seasonal Climate Update was jointly developed by the WMO Infrastructure (INFCOM) and Services (SERCOM) Commissions with contributions from:

- WMO Lead Centre for Long-Range Forecast Multi-Model Ensemble (LC-LRFMME), Korea Meteorological Administration, NOAA National Centers for Environmental Prediction
- WMO Global Producing Centres for Long-Range Forecast (GPCs-LRF): GPC-Beijing (China Meteorological Administration), GPC-CPTEC (Center for Weather Forecast and Climate Studies, Brazil), GPC-ECMWF (European Center for Medium-Range Forecast), GPC-Exeter (UK Met Office), GPC- Melbourne (Bureau of Meteorology), GPC-Montreal (Meteorological Services of Canada), GPC-Moscow (Hydro meteorological Center of Russia), GPC-Offenbach Deutscher Wetterdienst), GPC-Pretoria (South African Weather Services), GPC-Seoul (Korea Meteorological Administration), GPC-Tokyo (Japan Meteorological Agency), GPC-Toulouse (Météo-France), GPC-Washington (National Centers for Environmental Prediction), GPC-CMCC (Centro Euro-Mediterraneo sui Cambiamenti Climatici).

- International Research Institute for Climate and Society (IRI)